EVALUATION OF DEAD-END ULTRAFILTRATION PROPERTIES BY ULTRACENTRIFUGATION METHOD

EIJI IRITANI*, KOJI HATTORI
AND TOSHIRO MURASE
Department of Chemical Engineering, Nagoya University, Nagoya 464-01

Key Words: Membrane Separation, Filtration, Ultrafiltration, Ultracentrifugation, pH, Proteinaceous Solution, Density, Porosity, Dead-End Filtration, Upward Filtration

In protein ultrafiltration, solution environment factors such as pH and solvent density are important in controlling the filtration flux. Also, the properties of the filter cake of macromolecular solutes formed on the membrane surface play a vital role in determining the filtration flux in ultrafiltration. On the basis of the sedimentation velocity technique and the high-speed sedimentation equilibrium technique using an analytical ultracentrifuge, the influence of the protein solution pH on the time variation of the filtration flux in unstirred dead-end ultrafiltration was accurately described. It was clearly demonstrated that the low filtration flux around the isoelectric point is mainly due to the build-up of compact filter cake, which causes a large hydraulic flow resistance. Furthermore, it was shown that the solvent density ρ has a large effect on the dynamically balanced filtration rate in upward ultrafiltration just as it does on the sedimentation coefficient in ultracentrifugation.

Introduction

A dramatic flux decline during the ultrafiltration processes known as membrane fouling is the thorniest problem in the use of ultrafiltration systems. One of the critical factors governing such membrane fouling may be the formation of highly resistant filter cake caused by accumulation of the protein solutes on the membrane surface. Therefore, an understanding of the properties of the filter cake can serve as a basis for clarifying the real mechanism of ultrafiltration.

It is well known that the flux decline in protein ultrafiltration is markedly influenced by such factors of the solution environment as pH and the solution ionic strength[1-6,11,17,20]. We have recently determined that filtration characteristics under various solution conditions can be related to the properties of the filter cake formed on the membrane surface, determined by using a batchwise filter having sudden reduction in its filtration area[8]. Also, our previous studies have demonstrated that the density of the protein molecule is an important factor influencing the filtration flux in the recently developed upward ultrafiltration[7,9]. By studying the dependence of the filtration characteristics of protein ultrafiltration on pH and density of the solvent, insight will be gained into the importance of the various solution conditions.

In a previous paper[10], we attempted to evaluate the flux decline and the characteristic values of the filter cake by use of both the sedimentation velocity method and the high-speed sedimentation equilibrium method based on analytical ultracentrifugation. In this paper, the influences of pH on protein ultrafiltration are evaluated by use of ultracentrifugation data. Furthermore, by examining the dependence of sedimentation behavior in ultracentrifugation experiments regarding solvent density, the role of solvent density in dead-end upward ultrafiltration is discussed.

* Received October 20, 1993. Correspondence concerning this article should be addressed to E. Iritani.

1. Experimental Apparatus and Procedure

Ultrafiltration experiments were performed using an unstirred batch filtration device[8]. Dead-end ultrafiltration experiments were conducted under constant-pressure conditions controlled by a reducing valve by applying compressed nitrogen gas after the solutions were poured into the filter. The filtrate weight was measured with an electronic balance. The weights were converted to volumes using density correlations. In addition, upward ultrafiltration experiments[7,9] were performed, in which the filter was placed on an angled plate so that the filtrate flow was opposite to the direction of gravity. Asymmetric polysulfone membranes (PTTK) with a nominal molecular weight cut-off of 30,000 Da, supplied by Millipore Corp., were used for all ultrafiltration experiments.

The analytical ultracentrifugation experiments were conducted in a Hitachi Model 282 ultracentrifuge equipped with an optical system[10]. All experiments were performed at 293 K in a 1.5 or 12 mm double-sector centerpiece. The rotor speed was 55,000 or 60,000

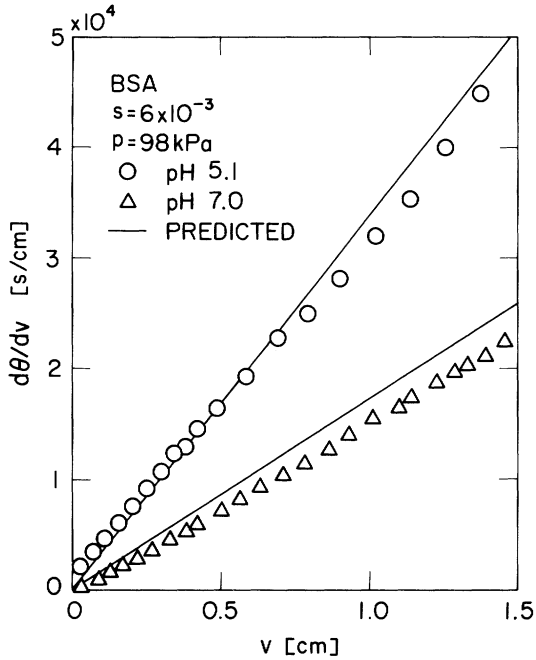

Fig. 1 Reciprocal filtration rate as function of filtrate volume per unit membrane area

min^{-1} in the sedimentation velocity experiment, and ranged from 45,000 to 60,000 min^{-1} in the high-speed sedimentation equilibrium experiment. The distributions of the concentration, the concentration gradient, and the refractive index gradient of the solution in the test cell were measured over time using both the ultraviolet scanner absorption system and Schlieren optics. In the sedimentation velocity experiment, the sedimentation coefficient was determined from the displacement of the sedimentation boundary, expressed as either the maximum in the concentration gradient curve or the refractive index gradient curve. In the high-speed sedimentation equilibrium experiment, the solutes sedimented at the cell bottom were gradually compressed to a minimum at a given constant rotor speed. The equilibrium thickness of the sediment of macromolecular solutes was measured after equilibrium was reached at a constant rotor speed. It was considered to be the distance from the cell bottom to the position of the maximum point in the concentration gradient curve nearest the cell bottom. The equilibrium thickness of the sediment was determined for a series of rotor speeds.

The macrosolute used in the experiments was bovine serum albumin (BSA) (Fraction V, Katayama Chemical Ind. Corp.) with a molecular weight of ca. 67,000 Da. BSA was dissolved in water prepared by an ultrapure water system for laboratory use (Puric-R, Olgano Corp.) with gentle agitation for a sufficient time (ca. 2 hr for all runs) to insure homogeneity at the desired concentration. The pH of the solution was adjusted downwards by the addition of 0.1 N HCl solution and upwards by the addition of 0.1 N NaOH solution. The density of the solvent was adjusted by adding appropriate amounts of sucrose, which has been widely used as an ideal gradient medium in density-gradient centrifugation.

2. Results and Discussion

2.1 Role of pH in ultrafiltration behavior

The experimental results of unstirred dead-end ultrafiltration for various values of solution pH are plotted in the form of the reciprocal filtration rate ($d\theta/dv$) versus the filtrate volume v per unit effective membrane area in **Fig. 1**. The filtration data yield straight lines in accordance with the cake filtration model[18,19] based on the build-up of a filter cake. The slope of the straight line at pH 5.1 — namely, the isoelectric point of BSA — is much steeper than that at pH 7. In other words, the filtration rate around the isoelectric point is much smaller than that at pH 7. Fane *et al.*[2-4,20] indicated that the dynamically balanced filtration rate in crossflow ultrafiltration shows a similar tendency. Also, we have previously shown that the average porosity ε_{av} of the filter cake of BSA formed on the membrane surface reaches its minimum and the average specific filtration resistance α_{av} reaches its maximum around the isoelectric pH, on the basis of unstirred dead-end ultrafiltration experiments using a batchwise filter which has an abrupt reduction in its filtration area[8]. The BSA molecule has a net positive charge at pH lower than isoelectric pH and a net negative charge at pH higher than isoelectric pH. As a result, the filter cake becomes loose and wet due to electrostatic repulsion between the charged BSA molecules. We will attempt to explain these phenomena quantitatively with the aid of analytical ultracentrifugation experiments. The solid lines in this figure indicate the theoretical predictions based on the ultracentrifugation data, as discussed below.

At relatively high solution concentrations there is an analogy between the sedimentation of a macromolecule in a solvent and the permeation of a solvent through the filter cake of macromolecules[14]. Thus the permeability data can be obtained from the sedimentation experiments. On the basis of the sedimentation velocity method using an analytical ultracentrifuge in which the motion of a solvent-solution boundary is followed, the local specific flow resistance α of the solvent flow through the interstices within individual macromolecules can be calculated as

$$\alpha = \frac{(\rho_s - \rho)\, r_i\, \Omega^2}{\mu \rho_s\, v_0} = \frac{\rho_s - \rho}{\mu \rho_s\, S} \tag{1}$$

where ρ_s is the density of the solutes, ρ is the density of the solvent, r_i is the radial distance of the sedimentation boundary from the center of rotation, Ω is the angular velocity of the rotor, μ is the viscosity of the solvent, v_0 is the sedimentation velocity, and S is the sedimentation coefficient.

Typical data for the sedimentation velocity method are shown as semi-log plots of r_i versus time θ in **Fig. 2**. The abscissa θ represents the time after the rotor speed

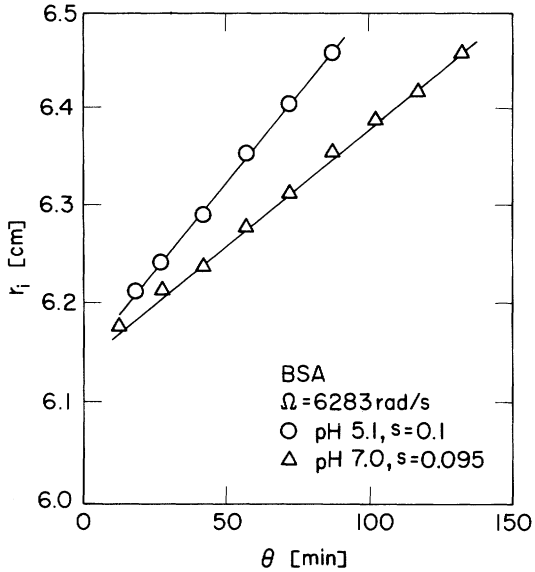

Fig. 2 Determination of sedimentation velocity in ultracentrifugation

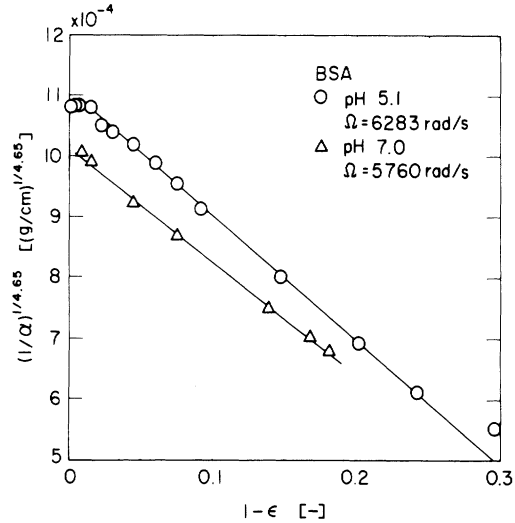

Fig. 3 Relation between local specific flow resistance and porosity of solution

has reached a constant value. It is apparent that the sedimentation velocity is constant under these experimental conditions because the plot shows a linear relationship. It is also apparent that the sedimentation velocity around the isoelectric point is much larger than that at pH 7 because the effects of charge on the sedimentation velocity can be negligible around the isoelectric pH[22].

On the basis of both the hindered sedimentation velocity equation describing gravity sedimentation presented by Michaels and Bolger[12] and Eq. (1), the relation between α and (1 - ε) may be written as

$$(1/\alpha)^{1/4.65} = \left(\frac{\rho_s d_f^2}{18 C_h}\right)^{1/4.65} \{1 - C_h(1-\varepsilon)\} \qquad (2)$$

where d_f is the average equivalent spherical diameter of solutes, C_h is the ratio of the volume of the hydrous protein molecule to the volume of the anhydrous protein molecule, and ε is the porosity of the solution. The relation between α and the volume fraction (1 - ε) of solutes in solution can be obtained by measuring the sedimentation velocities for a number of different solution concentrations.

In **Fig. 3**, the dependence of the local specific resistance on the solution concentration is plotted in the form of $(1/\alpha)^{1/4.65}$ versus (1 - ε). The plots are virtually linear as would be expected from Eq. (2). Interestingly, the values of the slopes are similar regardless of pH. It is apparent that α around the isoelectric point is much smaller than that at pH 7 at the same solution concentration (1 - ε).

Opong and Zydney[15] found that the hydraulic permeability of protein layers at physiologic ionic strength in ultrafiltration reached its maximum around the isoelectric point. Their results differ from ours[8]. They suggest that their permeability data of ultrafiltration can be explained qualitatively by the fact that the sedimentation coefficient was maximum around the isoelectric point. But their results of permeability are not correct due to the following considerations. We have previously found that the average specific filtration resistance α_{av} of the filter cake in ultrafiltration of BSA solutions reaches a definite maximum around the isoelectric point[8]. Fane reported similar results[4]. However, our results run counter to trends observed in sedimentation velocity data. Thus, these results cannot be explained simply by the data of the sedimentation coefficient. It is considered that the average specific filtration resistance depends largely on the porosity of the filter cake. If the most compact filter cake forms around the isoelectric point, the average specific filtration resistance of the filter cake around the isoelectric point may become larger than that at pH 7. Therefore, we attempted to conduct a high-speed sedimentation equilibrium experiment in order to evaluate the porosity of the filter cake.

If the solute concentration of the filter cake formed in ultrafiltration is known, then the specific flow resistance of the cake can be evaluated by using the permeability data at the corresponding concentration obtained by the sedimentation velocity method[14]. To treat the ultrafiltration problem quantitatively, it is necessary to evaluate the solute concentration of filter cake formed under various experimental conditions such as the filtration pressure, the solution concentration, and others. Therefore, it is of interest to examine the porosity of the filter cake formed at different values of pH. We thus determined the compression data representing the relation between the local porosity ε and the local solute compressive pressure p_s from high-speed sedimentation equilibrium experiments, in which a solution is subjected to a constant centrifugal field for a sufficient time. In the high-speed sedimentation equilibrium method, a compressed sediment can be formed at the cell bottom at a very high speed of ultracentrifugation.

If ε is related to p_s by Eq. (3), the equilibrium

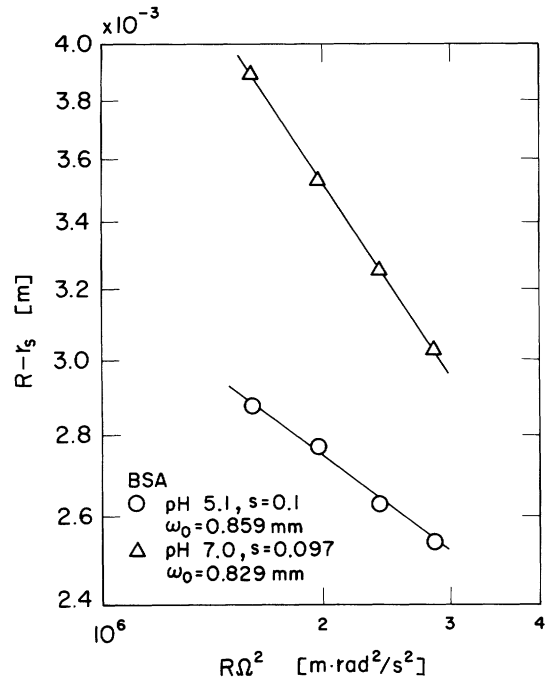

Fig. 4 Relation between equilibrium thickness of sediment and centrifugal acceleration

thickness (R - r_s) of the sediment is related to the centrifugal acceleration $R\Omega^2$ by Eq. (4)[10, 13].

$$1-\varepsilon = E\, p_s^{\beta} \quad p_s \geq p_{si} \tag{3}$$

$$R-r_s = \frac{\omega_o^{1-\beta}}{E(1-\beta)}\{(\rho_s-\rho)R\Omega^2\}^{-\beta} \tag{4}$$

where R is the distance from the center of rotation to the bottom of the sediment, r_s is the distance from the center of rotation to the surface of the sediment, and ω_0 is the net solute volume of the entire sediment per unit cross-sectional area. Below p_{si}, ε is assumed to be constant, and is equal to the porosity at pressure p_{si}.

Figure 4 represents the logarithmic plot of (R - r_s) against $R\Omega^2$. The plot shows a linear relationship in accordance with Eq. (4). It is of interest and significance that the sediment at the isoelectric point is much more compact than that at pH 7 because the BSA molecule carries no net charge at the isoelectric point. Therefore, it would be expected that in protein ultrafiltration a compact filter cake forms around the isoelectric point. Consequently, the average specific filtration resistance at the isoelectric point would become larger than at pH 7. The values of E and β in Eq. (4) can be determined from the plot in the figure. The relation between ε and p_s can then be obtained from Eq. (3). Since the dependence of α on ε can be evaluated from Eq. (2) using the sedimentation velocity data, α can be related to p_s. Since α and e [$= \varepsilon/(1-\varepsilon)$] are related to p_s, the distributions of the characteristic values of the filter cake can be evaluated on the basis of Eqs. (5) and (6) as described in some detail in a previous paper[10].

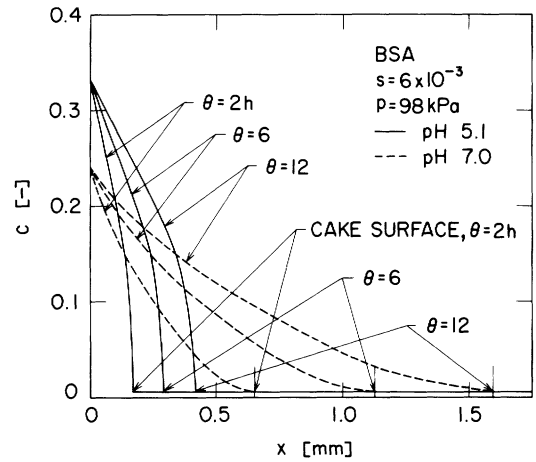

Fig. 5 Distribution of solute concentration in filter cake

$$1-\frac{p_s}{p} = \frac{\int_0^{\omega_{\omega_0}} \left(\frac{u}{u_1}\right)\alpha d\left(\frac{\omega}{\omega_0}\right)}{\int_0^{1} \left(\frac{u}{u_1}\right)\alpha d\left(\frac{\omega}{\omega_0}\right)} \tag{5}$$

$$\frac{u}{u_1} = 1-\frac{(e-e_{av.\,\omega})(m-1)}{e_{av}(1-ms)}\, s\,\frac{\omega}{\omega_0} \tag{6}$$

where e is the local void ratio (volume ratio of void to solute in filter cake), p is the applied filtration pressure, ω is the net solute volume per unit effective membrane area from the membrane up to an arbitrary position in the filter cake, u is the apparent solvent velocity relative to solute, u_1 is the filtration flux rate, $e_{av.\,\omega}$ is the average void ratio from the membrane surface to the distance ω from the membrane, m is the ratio of wet to dry cake mass, e_{av} is the average void ratio of entire filter cake, and s is the mass fraction of the solute in the solution. Thus the variations of the filtration flux rate can be determined from the compressible-cake resistance model, using the characteristic values of the filter cake[8, 10].

The variations of the mass fraction c of the solute across the filter cake calculated on the basis of the compressible-cake resistance model and the ultracentrifugation data are illustrated for different values of pH and filtration time θ in **Fig. 5**. In the compressible-cake resistance model, the solutes deposited on the membrane are treated as the filter cake, and this causes the hydraulic barrier. The cake tends to have a much more compact structure at the membrane in comparison to the relatively loose condition at the surface because the filter cake is compressible. Of considerable practical interest is that this result is in agreement with that obtained for cake filtration of particulate suspensions[21]. A much more compact filter cake exhibiting a large resistance to flow may form around the isoelectric point than that which forms at pH 7. Consequently, the filtration rate at the isoelectric point becomes lower than that at pH 7.

The solid lines in Fig. 1 indicate the theoretical prediction based on the compression-permeability data obtained in analytical ultracentrifugation. It was clearly demonstrated from both experiments and theory that the

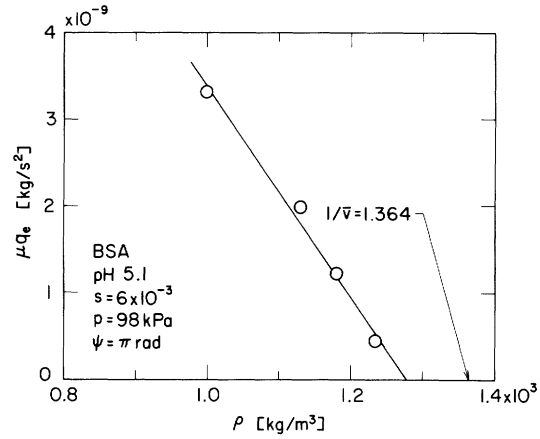

Fig. 6 μq_e versus ρ of solvent in upward ultrafiltration

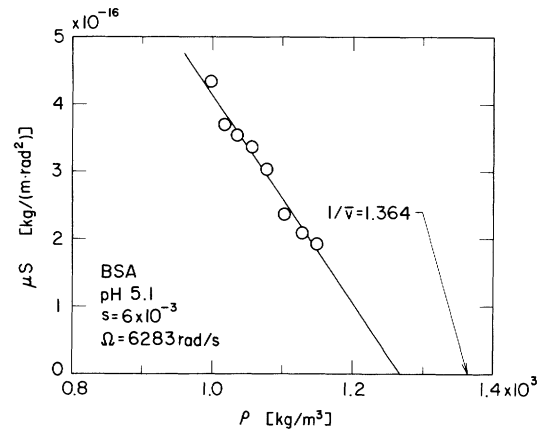

Fig. 7 μS versus ρ of solvent in ultracentrifugation

filtration rate around the isoelectric point is much lower than that at pH 7. At either pH the data are in relatively good agreement with the theory, indicating that the compressible-cake resistance model accurately describes the ultrafiltration behavior.

2.2 Role of solvent density in ultrafiltration behavior

In upward ultrafiltration, the density of the protein molecules is an important factor influencing the filtration characteristics, since the gravitational force acting on the protein molecules is the driving force in filter cake exfoliation. To probe the influence of solvent density on the dynamically balanced filtration rate in upward ultrafiltration, experiments were conducted for various values of the density ρ of the solvent[9]. The product of the dynamically balanced filtration rate q_e and the viscosity μ of the solvent is plotted against the density ρ of the solvent at pH 5.1 in **Fig. 6**. As can be seen, the plots are remarkably linear over the range studied. It is important to note that increases in ρ bring about decreases in μq_e. Dynamically balanced conditions in upward ultrafiltration may be achieved because the filter cake overlying the membrane is exfoliated continuously. Such a phenomenon appears to be caused by the gravitational force acting on the macrosolutes comprising the filter cake. Therefore, such an effect becomes more pronounced with smaller density of the solvent, leading to an increase in the difference between the density of the protein and that of the solvent. Extrapolation to $\mu q_e = 0$ leads to the value of the buoyant (effective) density ρ_b of the solute in its solution environment. The buoyant density of the protein solute is the actual density and includes hydration of the protein. The dry density of the solute, which is defined as the reciprocal of the partial specific volume $\bar{v}$, is reported to have the value of 1.364 g/cm^3 for BSA[16]. The buoyant density obtained from the upward ultrafiltration experiments is smaller than the dry density due to hydration of the protein. Also, we can obtain the buoyant density of the protein solute by ultracentrifugation experiments. In **Fig. 7**, the product of the sedimentation coefficient S in ultracentrifugation and the viscosity μ is plotted against the density ρ of the solvent. The plots are remarkably linear, as indicated by Eq. (1). Extrapolation to $\mu S = 0$ leads to the value of the buoyant density ρ_b of the solute. The most striking result is that this value is in excellent agreement with that obtained from the upward ultrafiltration experiments. This implies that there exists an analogy between the ultracentrifugation behavior and the upward ultrafiltration behavior.

Conclusions

To examine the effects of such factors of the solution environment as pH and the solvent density on the filtration characteristics of ultrafiltration of BSA solutions, ultracentrifugation experiments were conducted. Based on both the sedimentation velocity method and the high-speed sedimentation equilibrium method using analytical ultracentrifugation, variations of the filtration flux and the characteristics of the filter cake in ultrafiltration at various pH values were well evaluated. It was demonstrated from high-speed sedimentation equilibrium experiments that α depends on ε more strongly than pH for compressible cake, as BSA, and compact filter cake, which causes a large specific filtration resistance, forms around the isoelectric point. Consequently, the filtration rate around the isoelectric point became much lower than that at pH 7, regardless of a large sedimentation coefficient around the isoelectric point. In addition, the role of the solvent density in the dynamically balanced filtration rate in upward ultrafiltration was examined with the aid of sedimentation velocity experiments using an analytical ultracentrifuge. The value of the buoyant density obtained from the upward ultrafiltration experiments agreed well with that obtained from the ultracentrifugation experiments.

Acknowledgements

The authors would like to acknowledge the valuable help and advice of Hiroyuki Hattori, Hisashi Kojima and Yukiko Kabeya of The Center for Analytical Instruments, National Institute for Basic Biology with the ultracentrifugation experiments. This work has been supported by a Grant-in-Aid for Scientific Research from the Ministry of Education, Japan, Grant Nos. 03805089 and 04805098, and by the Asahi Glass Foundation.

Nomenclature

C_h	=	ratio of volume of hydrous protein molecule to volume of anhydrous protein molecule	[-]
c	=	mass fraction of solute in filter cake	[-]
d_f	=	average equivalent spherical diameter ofsolute	[m]
E	=	constant in Eq. (3)	[$Pa^{-\beta}$]
e	=	local void ratio	[-]
e_{av}	=	average void ratio of entire filter cake	[-]
$e_{av.\,\omega}$	=	void ratio from membrane surface to distance ω from membrane	[-]
m	=	ratio of wet to dry cake mass	[-]
p	=	applied filtration pressure	[Pa]
p_s	=	local compressive pressure acting on solute	[Pa]
p_{si}	=	pressure below which ε remains constant	[Pa]
q_e	=	dynamically balanced filtration rate	[m/s]
R	=	distance from center of rotation to bottom of sedimentation	[m]
r_i	=	radial distance of sedimentation boundary from center of rotation	[m]
r_s	=	distance from center of rotation to surface of sediment	[m]
S	=	sedimentation coefficient	[s/rad^2]
s	=	mass fraction of solute in solution	[-]
u	=	apparent solvent velocity relative to solute	[m/s]
u_1	=	filtration rate	[m/s]
v	=	filtrate volume per unit effective membrane area	[m]
v_0	=	sedimentation velocity	[m/s]
$\bar{v}$	=	partial specific volume	[m^3/kg]
x	=	distance from membrane surface	[m]
α	=	local specific filtration resistance	[m/kg]
α_{av}	=	average specific filtration resistance	[m/kg]
β	=	constant in Eq. (3)	[-]
ε	=	local porosity	[-]
ε_{av}	=	average porosity	[-]
θ	=	filtration or sedimentation time	[s]
μ	=	viscosity of solvent	[Pa·s]
ρ	=	density of solvent	[kg/m^3]
ρ_b	=	buoyant density of solute	[kg/m^3]
ρ_s	=	density of solute	[kg/m^3]
ψ	=	angle between filtrate flow and direction of gravity	[rad]
Ω	=	angular velocity	[rad/s]
ω	=	net solute volume per unit effective membrane area, from the membrane up to an arbitrary position in filter cake	[m]
ω_0	=	net solute volume of entire filter cake per unit effective membrane area	[m]

Literature Cited

1) Fane, A.G. and C.J.D. Fell: *AIChE Symp. Ser.*, **73** (163), 198-205 (1977)
2) Fane, A.G., C.J.D. Fell and A. Suki: *J. Membrane Sci.*, **16**, 195-210 (1983)
3) Fane, A.G., C.J.D. Fell and A.G. Waters: *J. Membrane Sci.*, **16**, 211-224 (1983)
4) Fane, A.G.: "Progress in Filtration and Separation 4, Ultrafiltration: Factors Influencing Flux and Rejection" (ed. by R.J. Wakeman), p. 134-139, Elsevier, Netherlands (1986)
5) Forbes, F.: *Chem. Eng.*, **257**, 29-34 (1972)
6) Hopfenberg, H.B., V.T. Stannett and M.W. Bailey: *AIChE Symp. Ser.*, **70** (139), 1-10 (1974)
7) Iritani, E., T. Watanabe and T. Murase: *Kagaku Kogaku Ronbunshu*, **17**, 206-209 (1991)
8) Iritani, E., S. Nakatsuka, H. Aoki and T. Murase: *J. Chem. Eng. Japan*, **24**, 177-183 (1991)
9) Iritani, E., T. Watanabe and T. Murase: *J. Membrane Sci.*, **69**, 87-97 (1992)
10) Iritani, E., K. Hattori and T. Murase: *J. Membrane Sci.*, **81**, 1-13 (1993)
11) Kim, K.J., P. Sun, V. Chen, D.E. Wiley and A.G. Fane: *J. Membrane Sci.*, **80**, 241-249 (1993)
12) Michaels, A.S. and J.C. Bolger: *Ind. Eng. Chem. Fundam.*, **1**, 24-33 (1962)
13) Murase, T., M. Iwata, T. Adachi, L. Gmachowski and M. Shirato: *J. Chem. Eng. Japan*, **22**, 378-384 (1989)
14) Nakao, S., J.G. Wijmans and C.A. Smolders: *J. Membrane Sci.*, **26**, 165-178 (1986)
15) Opong, W.S. and A.L. Zydney: *J. Colloid Interface Sci.*, **142**, 41-60 (1991)
16) Peters, T. Jr.: *Adv. Protein Chem.*, **37**, 161-245 (1985)
17) Rodgers, V.G. and R.E. Sparks: *J. Membrane Sci.*, **78**, 163-180 (1993)
18) Ruth, B.F.: *Ind. Eng. Chem.*, **27**, 708-723 (1935)
19) Ruth, B.F.: *Ind. Eng. Chem.*, **38**, 564-571 (1946)
20) Suki, A., A.G. Fane and C.J.D. Fell: *J. Membrane Sci.*, **21**, 269-283 (1984)
21) Tiller, F.M. and H. Cooper: *AIChE J.*, **8**, 445-449 (1962)
22) Van Holde, K.E.: "The Proteins, Third Ed., Vol. I, Chap. 4. Sedimentation Analysis of Proteins" (eds. by H. Neurath and R.L. Hill), p. 235-238, Academic Press, New York (1975)

(Presented at the 58th Annual Meeting of The Society of Chemical Engineers, Japan, at March, April, 1993.)